

Constituent quark model study of light- and strange-baryon spectra

A. Valcarce⁽¹⁾, H. Garcilazo⁽²⁾, J. Vijande⁽¹⁾

(1) *Grupo de Física Nuclear and IUFFyM,
Universidad de Salamanca, E-37008 Salamanca, Spain*

(2) *Escuela Superior de Física y Matemáticas,
Instituto Politécnico Nacional, Edificio 9, 07738 México D.F., Mexico*

Abstract

We investigate the structure of the $SU(3)$ octet and decuplet baryons employing a constituent quark model designed for the study of the baryon-baryon interaction and successfully applied to the meson spectra. The model considers through the interacting potential perturbative, one-gluon exchange, and non-perturbative, boson exchanges and confinement, aspects of the underlying theory, QCD. We solve the three-quark problem by means of the Faddeev method in momentum space. We analyze the effect of the different terms in the interaction and make contact with the use of relativistic kinematics. We find an explanation to the strong contribution of the pseudoscalar forces in the semirelativistic approach for the octet baryons. A phenomenological recipe for the regularization parameter of the one-gluon exchange is found.

Keywords:

nonrelativistic quark models, baryon spectra

Pacs:

12.39.Jh, 12.39.Pn, 14.20.-c

I. INTRODUCTION

The complexity of Quantum Chromodynamics (QCD), the quantum field theory of the strong interaction, has prevented so far a rigorous deduction of its predictions even for the simplest hadronic systems. In the meantime while lattice QCD starts providing reliable results, QCD-inspired models are useful tools to get some insight into many of the phenomena of the hadronic world. One of the central issues to be addressed is a quantitative description of the low-energy phenomena, from the baryon-baryon interaction to the baryon spectra, still one of the major challenges in hadronic physics.

The very success of QCD-inspired models supports the picture which has emerged from more fundamental studies, namely, that below a certain scale QCD is a weakly coupled theory with asymptotically free quark and gluon degrees of freedom, but above this scale a strong coupling regime emerges in which color is confined and chiral symmetry is broken. These two aspects, confinement and chiral symmetry breaking, are now recognized as basic ingredients in any QCD-inspired model for the low-energy (and therefore non-perturbative) sector. Along this line, the simplest approach is doubtless the constituent quark model, where multigluon degrees of freedom are eliminated in favor of confined constituent quarks with effective masses coming from chiral symmetry breaking and quark-quark effective interactions [1]. Although little is known about the mechanism which confines the quarks inside hadrons, unquenched lattice QCD suggests a linear potential screened at long-distances due to the creation of $q\bar{q}$ pairs out of vacuum [2]. Finally, much evidence has been accumulated about the importance of a color-spin force (as the one arising from the one-gluon exchange) in the low-energy hadron phenomenology [3].

Using these basic ingredients several quark models have been proposed in the literature [4]. In general, they were designed either for the study of the baryon-baryon interaction or the baryon spectra. For example, in Refs. [5–9] the two and/or the three-nucleon problem were studied in detail, while Refs. [10–15] made a thorough analysis of the baryon spectra. One of the most general conclusions arising from these works is that the study of a particular problem does not impose enough restrictions as to constrain neither the ingredients nor the parameters of the model. To our knowledge, in recent years the ambitious project of a simultaneous description of the baryon-baryon interaction and the baryon (and meson) spectra has only been undertaken by the constituent quark model of Refs. [16,17], applied within the same framework to the baryon-baryon interaction [16] as well as to the baryon spectra [17]. This model is based on the idea that the constituent quark mass appears because of the spontaneous breaking of the original chiral symmetry of the QCD Lagrangian, what generates boson-exchange interactions between quarks. Thus, the model takes into account perturbative and non-perturbative aspects of QCD through the one-gluon exchange and boson exchanges and confinement, respectively. It was originally designed to study the nonstrange sector and it has been recently generalized to all flavor sectors. It has already been applied to the meson spectra and baryon-baryon interaction with encouraging results [18,19].

Any phenomenological model should be tested against as many observables as possible to clearly understand its strengths and weakness, being this the only way one can extract reliable predictions. This is why in this work we pursue the description of the nonstrange and strange baryon spectra based on the constituent quark model of Ref. [18]. For this

purpose, we will start in the next section resuming its basic properties. In Sec. III we will briefly describe the Faddeev method in momentum space used to solve the three-body problem. Section IV will be devoted to present and discuss the results in comparison to other models in the literature. Finally, in Sec. V we will summarize our conclusions.

II. SU(3) CONSTITUENT QUARK MODEL

Let us outline the basic ingredients of the constituent quark model of Ref. [18]. Since the origin of the quark model hadrons have been considered to be built by constituent (massive) quarks. Nowadays it is widely recognized that the constituent quark mass appears because of the spontaneous breaking of the original chiral symmetry of the QCD Lagrangian, what gives rise to boson-exchange interactions between quarks. The quark-quark meson-exchange potentials are given by:

$$V_\chi(\vec{r}_{ij}) = V_\pi(\vec{r}_{ij}) + V_\sigma(\vec{r}_{ij}) + V_K(\vec{r}_{ij}) + V_\eta(\vec{r}_{ij}), \quad (1)$$

each contribution given by,

$$\begin{aligned} V_\pi(\vec{r}_{ij}) &= \frac{g_{ch}^2}{4\pi} \frac{m_\pi^2}{12m_i m_j} \frac{\Lambda_\pi^2}{\Lambda_\pi^2 - m_\pi^2} m_\pi \left[Y(m_\pi r_{ij}) - \frac{\Lambda_\pi^3}{m_\pi^3} Y(\Lambda_\pi r_{ij}) \right] (\vec{\sigma}_i \cdot \vec{\sigma}_j) \sum_{a=1}^3 (\lambda_i^a \cdot \lambda_j^a), \\ V_\sigma(\vec{r}_{ij}) &= -\frac{g_{ch}^2}{4\pi} \frac{\Lambda_\sigma^2}{\Lambda_\sigma^2 - m_\sigma^2} m_\sigma \left[Y(m_\sigma r_{ij}) - \frac{\Lambda_\sigma}{m_\sigma} Y(\Lambda_\sigma r_{ij}) \right], \\ V_K(\vec{r}_{ij}) &= \frac{g_{ch}^2}{4\pi} \frac{m_K^2}{12m_i m_j} \frac{\Lambda_K^2}{\Lambda_K^2 - m_K^2} m_K \left[Y(m_K r_{ij}) - \frac{\Lambda_K^3}{m_K^3} Y(\Lambda_K r_{ij}) \right] (\vec{\sigma}_i \cdot \vec{\sigma}_j) \sum_{a=4}^7 (\lambda_i^a \cdot \lambda_j^a), \\ V_\eta(\vec{r}_{ij}) &= \frac{g_{ch}^2}{4\pi} \frac{m_\eta^2}{12m_i m_j} \frac{\Lambda_\eta^2}{\Lambda_\eta^2 - m_\eta^2} m_\eta \left[Y(m_\eta r_{ij}) - \frac{\Lambda_\eta^3}{m_\eta^3} Y(\Lambda_\eta r_{ij}) \right] (\vec{\sigma}_i \cdot \vec{\sigma}_j) [\cos\theta_P (\lambda_i^8 \cdot \lambda_j^8) - \sin\theta_P], \end{aligned} \quad (2)$$

the angle θ_P appears as a consequence of considering the physical η instead the octet one. $g_{ch} = m_q/f_\pi$, the λ 's are the $SU(3)$ flavor Gell-Mann matrices. m_i is the quark mass and m_π , m_K and m_η are the masses of the $SU(3)$ Goldstone bosons, taken to be their experimental values. m_σ is determined through the PCAC relation $m_\sigma^2 \sim m_\pi^2 + 4m_{u,d}^2$ [20]. Finally, $Y(x)$ is the standard Yukawa function defined by $Y(x) = e^{-x}/x$.

QCD perturbative effects are taken into account through the one-gluon-exchange (OGE) potential [21]. The nonrelativistic reduction of the one-gluon-exchange diagram in QCD for point-like quarks presents a contact term that, when not treated perturbatively, leads to collapse [22]. This is why one maintains the structure of the OGE, but the δ function is regularized in a suitable way. This regularization, justified by the finite size of the systems studied, has to be flavor dependent [23]. As a consequence, the OGE reads,

$$V_{OGE}(\vec{r}_{ij}) = \frac{1}{4} \alpha_s \vec{\lambda}_i^c \cdot \vec{\lambda}_j^c \left\{ \frac{1}{r_{ij}} - \frac{1}{6m_i m_j} \vec{\sigma}_i \cdot \vec{\sigma}_j \frac{e^{-r_{ij}/r_0(\mu)}}{r_{ij} r_0^2(\mu)} \right\}, \quad (3)$$

where λ^c are the $SU(3)$ color matrices, α_s is the quark-gluon coupling constant, and $r_0(\mu) = \hat{r}_0 \mu_{nn}/\mu_{ij}$, where μ_{ij} is the reduced mass of quarks ij (n stands for the light u and d quarks) and \hat{r}_0 is a parameter to be determined from the data.

The strong coupling constant, taken to be constant for each flavor sector, has to be scale-dependent when describing different flavor sectors [24]. Such an effective scale dependence has been related to the typical momentum scale of each flavor sector assimilated to the reduced mass of the system [25]. This has been found to be relevant for the study of the meson spectra within the present model [18]. In our case, without being a relevant parameter, we will respect the nice determination established there,

$$\alpha_s(\mu) = \frac{\alpha_0}{\ln[(\mu^2 + \mu_0^2)/\gamma_0^2]}, \quad (4)$$

where μ is the reduced mass of the interacting qq pair and $\alpha_0 = 2.118$, $\mu_0 = 36.976$ MeV and $\gamma_0 = 0.113$ fm $^{-1}$. This equation gives rise to $\alpha_s \sim 0.54$ for the light-quark sector, a value consistent with the one used in the study of the nonstrange hadron phenomenology [16,17], $\alpha_s \sim 0.49$ for a light-strange pair and $\alpha_s \sim 0.44$ for the strange sector, and it also has an appropriate high Q^2 behavior, $\alpha_s \sim 0.127$ at the Z_0 mass [26]. In Fig. 1 we compare this parametrization to the experimental data [27] and to the parametrization obtained in Ref. [28] from an analytical model of QCD.

Finally, any model imitating QCD should incorporate confinement. Lattice calculations in the quenched approximation derived, for heavy quarks, a confining interaction linearly dependent on the interquark distance. The consideration of sea quarks apart from valence quarks (unquenched approximation) suggests a screening effect on the potential when increasing the interquark distance [2]. A screened potential simulating these results can be written as,

$$V_{CON}(\vec{r}_{ij}) = -a_c(1 - e^{-\mu_c r_{ij}})(\vec{\lambda}_i^c \cdot \vec{\lambda}_j^c) . \quad (5)$$

At short distances it presents a linear behavior with an effective confinement strength $a = a_c \mu_c \vec{\lambda}_i^c \cdot \vec{\lambda}_j^c$, while it becomes constant at large distances. Screened confining potentials have been analyzed in the literature providing an explanation to the missing state problem in the baryon spectra [29], improving the description of the heavy-meson spectra [30], and justifying the deviation of the meson Regge trajectories from the linear behavior for higher angular momentum states [31].

We have not considered the noncentral contributions arising from the different terms of the interacting potential. Experimentally, there is no evidence for important effects of the noncentral terms on the baryon spectra. This is clearly observed in the almost degeneracy of the nucleon ground states with $J^\pi = 1/2^-$ and $J^\pi = 3/2^-$, or their first excited states with the nucleon ground state with $J^\pi = 5/2^-$. The same is observed around the whole baryon spectra except for the particular problem of the relative large separation between the $\Lambda(1405)$, $J^\pi = 1/2^-$, and the $\Lambda(1520)$, $J^\pi = 3/2^-$, related to the vicinity of the $N\bar{K}$ threshold [32].

Theoretically, the spin-orbit force generated by the OGE has been justified to cancel with the Thomas precession term obtained from the confining potential [33]. This is not however the case for the two-baryon system where, by means of an explicit model for confinement, it has been demonstrated that the strong cancellation in the baryon spectra translates into a constructive effect for the two-baryon system [34]. One should notice that the scalar boson-exchange potential also presents a spin-orbit contribution with the same properties

as before, it cancels the OGE spin-orbit force in the baryon spectra while it adds to the OGE contribution for the nucleon-nucleon P -waves and cancels for D -waves [35], as it is observed experimentally. Such a different behavior in the one- and two-baryon systems is due to the absence of a direct term in the OGE spin-orbit force (due to the color of the gluon only quark-exchange diagrams are allowed), while the spin-orbit contribution of the confining interaction in Ref. [34] and that of the scalar boson-exchange potential in Ref. [35] are dominated by a direct term, without quark exchanges. Regarding the tensor terms of the meson-exchange potentials, they have been explicitly evaluated in the literature (in a model with stronger meson-exchange potentials) finding contributions not bigger than 25 MeV [36]. This is due to the fact that the tensor terms give their most important contributions at intermediate distances (of the order of 1-2 fm), due to the direct term in the quark-quark potential. The regularization of the boson-exchange potentials below the chiral symmetry breaking scale suppresses their contributions for the very small distances involved in the one-baryon problem. This allows to neglect the noncentral terms of the interacting potential that would provide with a fine tune of the final results and would make very much involved and time-consuming the solution of the three-body problem by means of the Faddeev method in momentum space we pretend to use.

Once perturbative (one-gluon exchange) and nonperturbative (confinement and chiral symmetry breaking) aspects of QCD have been considered, one ends up with a quark-quark interaction of the form,

$$V_{q_i q_j}(\vec{r}_{ij}) = V_{CON}(\vec{r}_{ij}) + V_{OGE}(\vec{r}_{ij}) + V_\chi(\vec{r}_{ij}) \quad (6)$$

III. THREE-BODY FORMALISM

If there are no tensor or spin-orbit forces the Faddeev equations for the bound-state problem of three quarks can be written as

$$\begin{aligned} \langle p_i q_i; \ell_i \lambda_i S_i T_i | \phi_i^{LST} \rangle = & \frac{1}{E - p_i^2/2\eta_i - q_i^2/2\nu_i} \sum_{j \neq i} \sum_{\ell_j \lambda_j S_j T_j} \frac{1}{2} \int_{-1}^1 d\cos\theta \int_0^\infty q_j^2 dq_j \\ & \times t_i^{\ell_i S_i T_i}(p_i, p'_i; E - q_i^2/2\nu_i) A_L^{\ell_i \lambda_i \ell_j \lambda_j}(p'_i q_i p_j q_j) \\ & \times \langle S_i T_i | S_j T_j \rangle_{ST} \langle p_j q_j; \ell_j \lambda_j S_j T_j | \phi_j^{LST} \rangle, \end{aligned} \quad (7)$$

where S_i and T_i are the spin and isospin of the pair jk while S and T are the total spin and isospin. ℓ_i (\vec{p}_i) is the orbital angular momentum (momentum) of the pair jk , λ_i (\vec{q}_i) is the orbital angular momentum (momentum) of particle i with respect to the pair jk , and L is the total orbital angular momentum. $\cos\theta = \vec{q}_i \cdot \vec{q}_j / (q_i q_j)$ while

$$\begin{aligned} \eta_i &= \frac{m_j m_k}{m_j + m_k}, \\ \nu_i &= \frac{m_i(m_j + m_k)}{m_i + m_j + m_k}, \end{aligned} \quad (8)$$

are the usual reduced masses. For a given set of values of LST the integral equations (7) couple the amplitudes of the different configurations $\{\ell_i \lambda_i S_i T_i\}$. The spin-isospin recoupling coefficients $\langle S_i T_i | S_j T_j \rangle_{ST}$ are given by

$$\begin{aligned} \langle S_i T_i | S_j T_j \rangle_{ST} &= (-)^{S_j + \sigma_j - S} \sqrt{(2S_i + 1)(2S_j + 1)} W(\sigma_j \sigma_k S \sigma_i; S_i S_j) \\ &\quad \times (-)^{T_j + \tau_j - T} \sqrt{(2T_i + 1)(2T_j + 1)} W(\tau_j \tau_k T \tau_i; T_i T_j), \end{aligned} \quad (9)$$

with σ_i and τ_i the spin and isospin of particle i , and W is the Racah coefficient. The orbital angular momentum recoupling coefficients $A_L^{\ell_i \lambda_i \ell_j \lambda_j}(p'_i q_i p_j q_j)$ are given by

$$\begin{aligned} A_L^{\ell_i \lambda_i \ell_j \lambda_j}(p'_i q_i p_j q_j) &= \frac{1}{2L + 1} \sum_{M m_i m_j} C_{m_i, M - m_i, M}^{\ell_i \lambda_i L} C_{m_j, M - m_j, M}^{\ell_j \lambda_j L} \Gamma_{\ell_i m_i} \Gamma_{\lambda_i M - m_i} \Gamma_{\ell_j m_j} \\ &\quad \times \Gamma_{\lambda_j M - m_j} \cos[-M(\vec{q}_j, \vec{q}_i) - m_i(\vec{q}_i, \vec{p}'_i) + m_j(\vec{q}_j, \vec{p}_j)], \end{aligned} \quad (10)$$

with $\Gamma_{\ell m} = 0$ if $\ell - m$ is odd and

$$\Gamma_{\ell m} = \frac{(-)^{(\ell+m)/2} \sqrt{(2\ell + 1)(\ell + m)!(\ell - m)!}}{2^\ell ((\ell + m)/2)! ((\ell - m)/2)!} \quad (11)$$

if $\ell - m$ is even. The angles (\vec{q}_j, \vec{q}_i) , (\vec{q}_i, \vec{p}'_i) , and (\vec{q}_j, \vec{p}_j) can be obtained in terms of the magnitudes of the momenta by using the relations

$$\begin{aligned} \vec{p}'_i &= -\vec{q}_j - \frac{\eta_i}{m_k} \vec{q}_i, \\ \vec{p}_j &= \vec{q}_i + \frac{\eta_j}{m_k} \vec{q}_j, \end{aligned} \quad (12)$$

where ij is a cyclic pair. The magnitude of the momenta p'_i and p_j , on the other hand, are obtained in terms of q_i , q_j , and $\cos\theta$ using Eqs. (12) as

$$\begin{aligned} p'_i &= \sqrt{q_j^2 + \left(\frac{\eta_i}{m_k}\right)^2 q_i^2 + \frac{2\eta_i}{m_k} q_i q_j \cos\theta}, \\ p_j &= \sqrt{q_i^2 + \left(\frac{\eta_j}{m_k}\right)^2 q_j^2 + \frac{2\eta_j}{m_k} q_i q_j \cos\theta}. \end{aligned} \quad (13)$$

Finally, the two-body amplitudes $t_i^{\ell_i S_i T_i}(p_i, p'_i; E - q_i^2/2\nu_i)$ are given by the solution of the Lippmann-Schwinger equation

$$\begin{aligned} t_i^{\ell_i S_i T_i}(p_i, p'_i; E - q_i^2/2\nu_i) &= V_i^{\ell_i S_i T_i}(p_i, p'_i) + \int_0^\infty p_i''^2 dp_i'' V_i^{\ell_i S_i T_i}(p_i, p_i'') \\ &\quad \times \frac{1}{E - p_i''^2/2\eta_i - q_i^2/2\nu_i} t_i^{\ell_i S_i T_i}(p_i'', p'_i; E - q_i^2/2\nu_i), \end{aligned} \quad (14)$$

with

$$V_i^{\ell_i S_i T_i}(p_i, p'_i) = \frac{2}{\pi} \int_0^\infty r_i^2 dr_i j_{\ell_i}(p_i r_i) V_i^{S_i T_i}(r_i) j_{\ell_i}(p'_i r_i). \quad (15)$$

and j_ℓ the spherical Bessel function.

In the case where the three quarks are identical (N and Ω) the three amplitudes ϕ_1^{LST} , ϕ_2^{LST} , and ϕ_3^{LST} in Eq. (7) are identical so that it reduces to

$$\begin{aligned}
\langle p_i q_i; \ell_i \lambda_i S_i T_i | \phi^{LST} \rangle = & \frac{1}{E - p_i^2/2\eta_i - q_i^2/2\nu_i} \sum_{\ell_j \lambda_j S_j T_j} \int_{-1}^1 d\cos\theta \int_0^\infty q_j^2 dq_j \\
& \times t_i^{\ell_i S_i T_i}(p_i, p'_i; E - q_i^2/2\nu_i) A_L^{\ell_i \lambda_i \ell_j \lambda_j}(p'_i q_i p_j q_j) \\
& \times \langle S_i T_i | S_j T_j \rangle_{ST} \langle p_j q_j; \ell_j \lambda_j S_j T_j | \phi^{LST} \rangle, \tag{16}
\end{aligned}$$

with $(-)^{\ell_i + S_i + T_i} = 1$ as required by the Pauli principle since the wave function is color antisymmetric.

In the case where two quarks are identical and one is different (Λ , Σ , and Ξ) only two amplitudes are independent. Assuming that particles 2 and 3 are identical and 1 is different, only the amplitudes ϕ_1^{LST} and ϕ_2^{LST} are independent and satisfy the coupled integral equations [37,38]

$$\begin{aligned}
\langle p_2 q_2; \ell_2 \lambda_2 S_2 T_2 | \phi_2^{LST} \rangle = & G \frac{1}{E - p_2^2/2\eta_2 - q_2^2/2\nu_2} \sum_{\ell_3 \lambda_3 S_3 T_3} \frac{1}{2} \int_{-1}^1 d\cos\theta \int_0^\infty q_3^2 dq_3 \\
& \times t_2^{\ell_2 S_2 T_2}(p_2, p'_2; E - q_2^2/2\nu_2) A_L^{\ell_2 \lambda_2 \ell_3 \lambda_3}(p'_2 q_2 p_3 q_3) \\
& \times \langle S_2 T_2 | S_3 T_3 \rangle_{ST} \langle p_3 q_3; \ell_3 \lambda_3 S_3 T_3 | \phi_2^{LST} \rangle \\
+ & \frac{1}{E - p_2^2/2\eta_2 - q_2^2/2\nu_2} \sum_{\ell_1 \lambda_1 S_1 T_1} \frac{1}{2} \int_{-1}^1 d\cos\theta \int_0^\infty q_1^2 dq_1 \\
& \times t_2^{\ell_2 S_2 T_2}(p_2, p'_2; E - q_2^2/2\nu_2) A_L^{\ell_2 \lambda_2 \ell_1 \lambda_1}(p'_2 q_2 p_1 q_1) \\
& \times \langle S_2 T_2 | S_1 T_1 \rangle_{ST} \langle p_1 q_1; \ell_1 \lambda_1 S_1 T_1 | \phi_1^{LST} \rangle, \tag{17}
\end{aligned}$$

$$\begin{aligned}
\langle p_1 q_1; \ell_1 \lambda_1 S_1 T_1 | \phi_1^{LST} \rangle = & \frac{1}{E - p_1^2/2\eta_1 - q_1^2/2\nu_1} \sum_{\ell_2 \lambda_2 S_2 T_2} \int_{-1}^1 d\cos\theta \int_0^\infty q_2^2 dq_2 \\
& \times t_1^{\ell_1 S_1 T_1}(p_1, p'_1; E - q_1^2/2\nu_1) A_L^{\ell_1 \lambda_1 \ell_2 \lambda_2}(p'_1 q_1 p_2 q_2) \\
& \times \langle S_1 T_1 | S_2 T_2 \rangle_{ST} \langle p_2 q_2; \ell_2 \lambda_2 S_2 T_2 | \phi_2^{LST} \rangle, \tag{18}
\end{aligned}$$

where the identical-particles phase G is

$$G = (-1)^{1 + \ell_2 + \sigma_1 + \sigma_3 - S_2 + \tau_1 + \tau_3 - T_2}. \tag{19}$$

Substituting Eq. (18) into Eq. (17) one obtains a single integral equation for the amplitude ϕ_2^{LST} . Again, in the case of identical pairs one has $(-)^{\ell_1 + S_1 + T_1} = 1$.

The nonrelativistic Faddeev method has a problem if the two-body interactions allow transitions of the form $a + b \rightarrow c + d$, i.e., if the particles in the final state are different from the ones in the initial state. In that case the center of mass energy is different in the initial and final states. This problem, however, does not arise in our model since our two-body interactions given by Eq. (6) only allow transitions of the form $n + n \rightarrow n + n$, $n + s \rightarrow n + s$, and $s + s \rightarrow s + s$, n standing for a light u or d quark. The center of mass ambiguity in the case of transitions of the form $a + b \rightarrow c + d$ does not arise in the relativistic version of the Faddeev method described in Ref. [39].

IV. RESULTS AND DISCUSSION

The results we are going to present have been obtained by solving exactly the Schrödinger equation by the Faddeev method in momentum space we have just described. For baryons made up of three identical quarks we have also calculated the spectra by means of the hyperspherical harmonic (HA) expansion method [40]. The HA treatment allows a more intuitive understanding of the wave functions in terms of the hyperradius of the whole system. These wave functions will be used to calculate the root mean square radius. As a counterpart one has to go to a very high order in the expansion to get convergence. To assure this we shall expand up to $K = 24$ (K being the great orbital determining the order of the expansion). Differences in the results for the $3q$ bound state energies obtained by means of the two methods turn out to be at most of 5 MeV.

As mentioned above we will not perform a systematic study in order to determine the best set of parameters to fit the baryon spectra. Instead, we will start from the parameters used in Ref. [18] for the description of the meson spectra that are resumed in Table I. There are two parameters that may differ from the meson case, they are: \hat{r}_0 , connected to the typical size of the system where the contact interaction is regularized and a_c , the strength of confinement. We fix a_c to drive the Roper of the nucleon to its correct position. One could also have chosen to fix the negative parity states knowing the sensitivity of the Roper resonance to the kinematics used [41,42], however we prefer to maintain the same prescription as in the study of the nonstrange baryon spectra [17], to guarantee that a similar description is obtained for the light baryons. We fix \hat{r}_0 to have the correct $\Delta - N$ mass difference. Once we determine \hat{r}_0 for the light baryons, its value is determined for all other flavor sectors through the relation given in Sec. II, obtaining a correct description of all hyperfine splittings. Finally, we made a fine tune of the strange quark mass to improve the description of the ground states with strangeness different from zero.

Our results are shown in Fig. 2 for the different octet and decuplet baryons. As can be seen our election of fixing a_c to reproduce the Roper resonance gives, in general, masses somewhat smaller than experiment. As explained above, we could equally have determined a_c to describe the negative parity states producing a much better fit of the baryon spectra except for the Roper resonance, that it is know to decrease in energy when a semirelativistic prescription is used [42]. Let us focus our attention on several particular aspects that deserve a detailed discussion. A widely discussed issue on the baryon spectra has been the so-called level ordering problem. It can be easily illustrated for the nucleon spectrum in the pure harmonic limit. The $N^*(1440)$ $J^P = 1/2^+$ belongs to the $[56, 0^+]$ $SU(6)_{FS} \times O(3)$ irreducible representation and it appears in the $N = 2$ band, while the $N^*(1535)$ $J^P = 1/2^-$ belongs to the $[70, 1^-]$ appearing in the $N = 1$ band. As a consequence, the $N^*(1440)$ has $2\hbar\omega$ energy excitation while the $N^*(1535)$ has only $1\hbar\omega$ energy excitation, opposite to the order observed experimentally. Theoretically, this situation has been cured by means of appropriate phenomenological interactions as it is the case of anharmonic terms [3], scalar three-body forces [12], or pseudoscalar interactions [14,17].

The mechanism producing the reverse of the ordering between the positive and negative parity excited states is the following. In the case of the scalar three-body force of Ref. [12], in the limit of zero range it would act only for states whose wave function do not cancel at the origin. It therefore influences the $L = 0$ ground states and their radial excitations, while

producing essentially no effect for states with mixed symmetry (negative parity states). As a consequence, if this force is chosen attractive, it explains why the Roper resonances are lower than the negative parity excited states. In the case of the chiral pseudoscalar interaction, its $(\vec{\sigma} \cdot \vec{\sigma})(\vec{\lambda} \cdot \vec{\lambda})$ structure gives attraction for symmetric spin-flavor pairs and repulsion for antisymmetric ones. This lowers the position of the first radial excitation, with a completely symmetric spin-flavor wave function, with regard to the first negative parity state, with a spin-flavor mixed symmetry wave function. This effect appears in our model mainly through the one-pion and one-kaon exchange contributions. It has been illustrated in Fig. 3, where we plot the mass of the first radial and orbital excitations of the $\Sigma(1/2^+)$ as a function of the cutoff mass of the one-pion and one-kaon exchange potentials. The contribution of the pseudoscalar interactions is increased by letting the cutoff parameters $\Lambda_{\pi,K}$ to grow in the same manner $\Lambda'_{\pi,K} = \Lambda_{\pi,K} + \Lambda_0$. As can be seen, the reverse of the ordering between the positive and negative parity excited states is obtained for Λ_0 sufficiently large (around 3.2 fm^{-1} , $\Lambda_{\pi} = 7.4 \text{ fm}^{-1}$ and $\Lambda_K = 8.4 \text{ fm}^{-1}$). A model with such a strong cutoffs would not be realistic because the decuplet-octet [$\Sigma(3/2^+) - \Sigma(1/2^+)$] mass difference would be much larger than the experimental value. This difficulty is known to have a well defined and simple solution, due to the decreasing of the excitation energy of the nucleon Roper resonance induced by the relativistic kinematics [41,42], which would reduce the value of the cutoff needed.

Although the level ordering problem has been solved by potential models based only on pseudoscalar forces combined with relativistic kinematics, they give rise to very small sizes for baryons. We compare in Table II the root mean square radii obtained with the constituent quark model used in this work to those of Ref. [12], making use of a scalar three-body force, Ref. [15], based only on pseudoscalar forces and relativistic kinematics, and Ref. [11] based on the Bhaduri potential. Ref. [12] gives a very small size for the nucleon while Ref. [15] finds small sizes for all baryons. The model based on the Bhaduri potential [11] produces sizes closer to our model. These results can be understood in the following way. As explained above, the scalar three-body force of Ref. [12] gives a strong attraction for the nucleon and its radial excitations, being the responsible for their small radius, while it produces practically no effect on the other baryons, being their radius much bigger and comparable to those of Ref. [11]. In Ref. [15], the contribution of the pseudoscalar boson exchanges to the baryon masses (see Table II of Ref. [15]) is very large, specially for the octet baryons, being the responsible for their small sizes. Although for the decuplet baryons this contribution is reduced, the sizes obtained are still very small. As we will explain below this is a direct consequence of smearing out the pseudoscalar meson exchange delta function with a large cutoff. This is reflected, for example, in the mass difference induced by the one-pion and one-kaon exchanges between decuplet and octet baryons, $\Delta - N$, $\Sigma(3/2^+) - \Sigma(1/2^+)$, $\Xi(3/2^+) - \Xi(1/2^+)$, of the order of 900 MeV.

In the constituent quark model used in this work the hyperfine splitting is shared between pseudoscalar forces and perturbative QCD contributions, provided by the one-gluon exchange. In Table III we give the contribution of different pieces of the interacting hamiltonian to the energy of several octet and decuplet baryons. One observes that the hyperfine splittings are basically controlled by the OGE (V_2) and OPE (V_3) [OKE (V_5)] potentials in the non-strange [strange] sector. When the OGE and OPE are considered altogether (V_4) the splitting is bigger than the sum of both contributions separately, and they generate almost

the experimental hyperfine splitting, the η and σ given a final small tune. The expectation value of the OPE flavor operator for two light quarks,

$$\langle [f_{ij}]_F T_{ij} | \sum_{a=1}^3 \lambda_i^a \lambda_j^a | [f_{ij}]_F T_{ij} \rangle = \begin{cases} 1 & \text{if } [2]_F, T_{ij} = 1 \\ -3 & \text{if } [11]_F, T_{ij} = 0 \end{cases} \quad (20)$$

is replaced by the similar effect of the OKE when a light and a strange quarks are involved

$$\langle [f_{ij}]_F T_{ij} | \sum_{a=4}^7 \lambda_i^a \lambda_j^a | [f_{ij}]_F T_{ij} \rangle = \begin{cases} 2 & \text{if } [2]_F, T_{ij} = 1/2 \\ -2 & \text{if } [11]_F, T_{ij} = 1/2 \end{cases} \quad (21)$$

being $[f_{ij}]_F$ the flavor permutational symmetry in the quark pair (i, j) and T_{ij} the total isospin of the pair state. They enhance in a similar way the hyperfine splitting produced by the OGE: the OPE for light quark pairs and the OKE for light-strange ones. The important effect of the OGE is observed when Table III is compared to Table II of Ref. [15], the contribution of the pseudoscalar forces is much smaller in our case, generating decuplet-octet mass differences of the order of 100–200 MeV, the remaining mass difference given by the OGE. As a consequence the radii predicted are also bigger.

This regularization effect of the OGE over the pseudoscalar forces for the baryon spectra has been also observed in two-baryon calculations [43] (that we consider should be proximately linked to the one-body problem). A too strong nucleon-nucleon pseudoscalar force was found for models based only in Goldstone boson exchanges and, at the same time, they do not present the required attraction to reproduce the experimental data [43]. The consideration of the scalar octet of Goldstone bosons [44] (as proposed long ago in the first work of Ref. [16]) may remedy the situation for the two-body sector, but it is incompatible with the description of the baryon spectra, because it makes the system to collapse [15]. The reason for that can be easily understood looking at the results of Ref. [39], where it has been demonstrated that a different regularization scale is obtained for the same interaction when nonrelativistic or relativistic kinematics are used. A larger value of the regularization parameter of the OGE delta function was obtained for the case of the semirelativistic calculation (see Fig. 1 of Ref. [39]). Therefore, the regularization process of any delta function (as the ones present in the Goldstone boson exchanges) should be done with great care. The semirelativistic kinematics cannot be implemented without worrying about the corrections to the meson-exchange potential in a consistent way. Replacing the nonrelativistic by the semirelativistic kinematics, the value of the delta-function regularization parameter giving rise to unstable results is increased, the other way around, for the same regularization parameter the interaction is made much more stronger. In the presence of so a strong pseudoscalar force, as shown in the results of Ref. [15], the additional attraction provided by the scalar potential gives rise to collapse. This is not again the case of our model where the scalar interaction is crucial to understand simultaneously the one and the two-baryon problems and its strength is compatible with the description of both sectors [42], the one-gluon exchange being basic for these results. The same conclusion was obtained for the light baryons when the semirelativistic prescription was used [42].

Let us finally face the problem of the regularization parameter of the OGE, r_0 . As explained in Sec. II this parameter is taken to be flavor dependent, scaling with the reduced mass of the interacting quarks. The larger the system (the lighter the masses of the quarks

involved) the larger the value of r_0 that can be used without risk of collapse. In Fig. 4 we plot the mass of two $1/2^+$ ground states, N and Ξ , and two $3/2^+$ ground states, Δ and Ω , as a function of \hat{r}_0 . In the last two cases the completely symmetric spin-flavor wave function makes the OGE to be repulsive and therefore no important effect is observed independently of the flavor quark substructure. However, for the $1/2^+$ ground states the OGE gives attraction and the regularization should be done with care. We observe how the masses of the $N(1/2^+)$ and the $\Xi(1/2^+)$ start to decrease very rapidly for almost the same value of \hat{r}_0 (for $\hat{r}_0 = 0.1$ fm, marked as a vertical dashed line in the figure, both states have diminished around 500–600 MeV with respect to their asymptotic value). One should note that the value of r_0 for pairs containing strange quarks is much smaller, for example $\hat{r}_0 = 0.35$ fm implies $r_0^{nn} = 0.35$ fm while $r_0^{ns} = 0.28$ fm and $r_0^{ss} = 0.22$ fm. This flavor dependence combined with the effect of the pseudoscalar forces provides with a correct description of the hyperfine splittings, giving confidence to the election of the flavor dependence of the OGE regularization parameter.

V. SUMMARY

We have used a constituent quark model incorporating the basic properties of QCD to study the strange and nonstrange baryon spectra. The model takes into account the most important QCD nonperturbative effects: chiral symmetry breaking and confinement as dictated by unquenched lattice QCD. It also considers QCD perturbative effects through a flavor dependent one-gluon exchange potential. The parameters of the model are mostly fixed from other observables as the meson spectra or the baryon-baryon interaction.

The SU(3) three-body problem has been for the first time exactly solved by means of the Faddeev method in momentum space, obtaining results of similar quality to others present in the literature based on models specifically designed for the study of the baryon spectra. The model provides with baryon root mean square radii much bigger than models based only in pseudoscalar boson exchanges. This is a consequence of the reduced contribution of the pseudoscalar forces due to the presence of the one-gluon exchange. These pseudoscalar forces are important for the correct position of the positive and negative parity excited states in all flavor sectors, but they should not be artificially strengthened making the systems highly unstable. The Roper resonances are known to be sensitive to relativistic kinematics, and therefore a reduced contribution of the pseudoscalar forces should be enough to solve the so-called level ordering problem. The presence of the scalar Goldstone boson exchanges, crucial to make contact with the two-body problem, would not be compatible with a strong pseudoscalar contribution.

We have analyzed the dependence of the spectra on the regularization parameter of the OGE, obtaining a pretty good agreement with a scale dependence based on the reduced mass of the interacting quarks. This OGE potential gives an important contribution to the decuplet-octet mass difference being basic to regularize the pseudoscalar forces needed.

Finally, although we do not believe that explanations based on constituent quark models may rule out or contradict other alternative ones, one should acknowledge the capability of constituent quark models for a coherent understanding of the low-energy phenomena of the baryon spectroscopy and the baryon-baryon interaction in a simple framework based on the

contribution of pseudoscalar, scalar and one-gluon-exchange forces between quarks.

VI. ACKNOWLEDGMENTS

This work has been partially funded by Ministerio de Ciencia y Tecnología under Contract No. FPA2004-05616, by Junta de Castilla y León under Contract No. SA-104/04, and by COFAA-IPN (México).

REFERENCES

- [1] A. Manohar and V. Georgi, Nucl. Phys. B **234**, 189 (1984).
- [2] G.S. Bali, Phys. Rep. **343**, 1 (2001).
- [3] N. Isgur, Phys. Rev. D **62**, 054026 (2000); nucl-th/0007008.
- [4] A. Valcarce, H. Garcilazo, F. Fernández, and P. González, Rep. Prog. Phys. **68**, 965 (2005).
- [5] K. Shimizu, Rep. Prog. Phys. **52**, 1 (1989).
- [6] K. Bräuer, A. Faessler, F. Fernández, and K. Shimizu, Nucl. Phys. A **507** 599 (1990).
- [7] F. Wang, G.H. Wu, L.J. Teng, and T. Goldman, Phys. Rev. Lett. **69**, 2901 (1992).
- [8] Y.W. Yu, Z.Y. Zhang, P.N. Shen, and L.R. Dai, Phys. Rev. C **52**, 3393 (1995).
- [9] Y. Fujiwara, C. Nakamoto, and Y. Suzuki, Phys. Rev. C **54**, 2180 (1996). Y. Fujiwara, T. Fujita, M. Kohno, C. Nakamoto, and Y. Suzuki, Phys. Rev. C **65**, 014002 (2002).
- [10] N. Isgur and G. Karl, Phys. Rev. D **18**, 4187 (1978); *ibid* **19**, 2653 (1979); *ibid* **20**, 1191 (1979). S. Capstick and N. Isgur, Phys. Rev. D **34**, 2809 (1986).
- [11] B. Silvestre-Brac and C. Gignoux, Phys. Rev. D **32**, 743 (1985).
- [12] B. Desplanques, C. Gignoux, B. Silvestre-Brac, P. González, J. Navarro, and S. Noguera, Z. Phys. A **343**, 331 (1992).
- [13] Z. Dziembowski, M. Fabre de la Ripelle, and G.A. Miller, Phys. Rev. C **53**, R2038 (1996).
- [14] L.Ya. Glozman and D.O. Riska, Phys. Rep. **268**, 263 (1996).
- [15] M. Furuichi and K. Shimizu, Phys. Rev. C **65**, 025201 (2002).
- [16] F. Fernández, A. Valcarce, U. Straub, and A. Faessler, J. Phys. G **19**, 2013 (1993). D.R. Entem, F. Fernández, and A. Valcarce, Phys. Rev. C **62**, 034002 (2000). B. Juliá-Díaz, J. Haidenbauer, A. Valcarce, and F. Fernández, Phys. Rev. C **65**, 034001 (2002).
- [17] H. Garcilazo, A. Valcarce, and F. Fernández, Phys. Rev. C **63**, 035207 (2001); *ibid* **64**, 058201 (2001).
- [18] J. Vijande, F. Fernández, and A. Valcarce, J. Phys. G **31**, 481 (2005).
- [19] T. Fernández-Caramés, A. Valcarce, H. Garcilazo, and P. González, Phys. Lett. B, submitted (2005).
- [20] M.D. Scadron, Phys. Rev. D **26**, 239 (1982).
- [21] A. de Rújula, H. Georgi, and S.L. Glashow, Phys. Rev. D **12**, 147 (1975).
- [22] R.K. Bhaduri, L.E. Cohler, and Y. Nogami, Phys. Rev. Lett. **44**, 1369 (1980).
- [23] J. Weinstein and N. Isgur, Phys. Rev. D **27**, 588 (1983).
- [24] S. Titard and F.J. Yndurain, Phys. Rev. D **51**, 6348 (1995). A.M. Badalian and B.L.G. Bakker, Phys. Rev. D **62**, 094031 (2000).
- [25] F. Halzen, C. Olson, M.G. Olsson and M.L. Stong, Phys. Rev. D **47**, 3013 (1993).
- [26] C.T.H. Davies *et al.*, Phys. Rev. D **56**, 2755 (1997).
- [27] S. Kluth, hep-ex/0309070. P. Achard *et al.*, Phys. Lett. B **536**, 217 (2002).
- [28] D.V. Shirkov and I.L. Solovtsov, Phys. Rev. Lett. **79**, 1209 (1997).
- [29] J. Vijande, P. González, H. Garcilazo, and A. Valcarce, Phys. Rev. D **69**, 074019 (2004).
- [30] P. González, A. Valcarce, H. Garcilazo, and J. Vijande, Phys. Rev. D **68**, 034007 (2003).
- [31] M.M. Brisudová, L. Burakovsky, and T. Goldman, Phys. Rev. D **61**, 054013 (2000).
- [32] E.A. Veit, B.K. Jennings, A.W. Thomas, and R.C. Barrett, Phys. Rev. D **31**, 1033 (1985).

- [33] N. Isgur, Phys. Rev. D **62** 014025 (2000).
- [34] Y. Koike, Nucl. Phys. A **454** 509 (1986). Y. Koike, O. Morimatsu, and K. Yazaki, Nucl. Phys. A **449** 635 (1986).
- [35] A. Valcarce, A. Buchmann, F. Fernández, and A. Faessler, Phys. Rev. C **51**, 1480 (1995).
- [36] M. Furuichi, K. Shimizu, and S. Takeuchi, Phys. Rev. C **68**, 034001 (2003).
- [37] I. R. Afnan and A. W. Thomas, Phys. Rev. C **10**, 109 (1974).
- [38] H. Garcilazo and T. Mizutani, *πNN Systems* (World Scientific, Singapore, 1990).
- [39] H. Garcilazo, Phys. Rev. C **67**, 055203 (2003); *ibid* **71**, 045204 (2005).
- [40] N. Barnea, W. Leidemann, and G. Orlandini, Phys. Rev. C **61**, 054001 (2000).
- [41] J. Carlson, J. Kogut, and V.R. Pandharipande, Phys. Rev. D **27**, 233 (1983).
- [42] H. Garcilazo and A. Valcarce, Phys. Rev. C **68**, 035207 (2003).
- [43] C. Nakamoto and H. Toki, Prog. Theor. Phys. **99**, 1001 (1998).
- [44] D. Bartz and Fl. Stancu, Nucl. Phys. A **688**, 915 (2001).

TABLES

TABLE I. Quark-model parameters.

Quark masses	$m_u = m_d$ (MeV)	313
	m_s (MeV)	500
Goldstone bosons	m_π (fm ⁻¹)	0.70
	m_σ (fm ⁻¹)	3.42
	m_η (fm ⁻¹)	2.77
	m_K (fm ⁻¹)	2.51
	$\Lambda_\pi = \Lambda_\sigma$ (fm ⁻¹)	4.20
	$\Lambda_\eta = \Lambda_K$ (fm ⁻¹)	5.20
	$g_{ch}^2/(4\pi)$	0.54
	θ_P (°)	-15
Confinement	a_c (MeV)	230
	μ_c (fm ⁻¹)	0.70
OGE	\hat{r}_0 (fm)	0.35

TABLE II. Root mean square radii, $\langle r^2 \rangle^{1/2}$ in fm, of states of identical particles obtained with our model (CCQM), compared to Ref. [12], considering a scalar three-body force, Ref. [15], based only on pseudoscalar boson exchanges and relativistic kinematics, and Ref. [11] based on a OGE potential.

State	CCQM	Ref. [12]	Ref. [15]	Ref. [11]
$N(1/2^+)$	0.482	0.38	0.304	0.467
$N^*(1/2^+)$	0.961	0.79	0.463	-
$N(1/2^-)$	0.829	0.78	-	-
$\Delta(3/2^+)$	0.635	0.51	0.390	0.537
$\Delta^*(3/2^+)$	1.149	0.90	0.534	-
$\Omega(3/2^+)$	0.513	-	0.395	0.418
$\Omega^*(3/2^+)$	0.897	-	0.543	-

TABLE III. Eigenvalue, in MeV, of the kinetic energy combined with different contributions of the interacting potential. The subindexes in the potential stand for: 1 = CON , 2 = $CON + OGE$, 3 = $CON + \pi$, 4 = $CON + OGE + \pi$, 5 = $CON + OGE + \pi + K$, 6 = $CON + OGE + \pi + K + \eta$, 7 = $CON + OGE + \pi + K + \eta + \sigma$.

State	V_1	V_2	V_3	V_4	V_5	V_6	V_7
$N(1/2^+)$	1534	1254	1407	969	969	1030	939
$\Delta(3/2^+)$	1534	1314	1510	1291	1291	1283	1232
$N^*(1/2^+)$	1787	1601	1716	1448	1448	1479	1435
$N(1/2^-)$	1722	1530	1675	1422	1422	1447	1411
$\Sigma(1/2^+)$	1679	1417	1674	1408	1326	1229	1213
$\Sigma(3/2^+)$	1679	1462	1673	1454	1437	1438	1382
$\Sigma^*(1/2^+)$	1983	1757	1931	1752	1703	1688	1644
$\Sigma(1/2^-)$	1859	1677	1854	1671	1645	1634	1598
$\Lambda(1/2^+)$	1679	1405	1600	1225	1171	1217	1122
$\Xi(1/2^+)$	1819	1557	1819	1557	1472	1446	1351
$\Omega(3/2^+)$	1955	1743	1955	1743	1743	1728	1650

FIGURES

FIG. 1. Effective scale-dependent strong coupling constant α_s given in Eq. (4) as a function of momentum. The solid line represents our parametrization. Dots and triangles are the experimental results of Refs. [27]. We plot by a dashed line the parametrization obtained in Ref. [28] using $\Lambda = 0.2$ GeV.

FIG. 2. Relative energy (a) N and Δ , (b) Λ and Σ , (c) Ξ and Ω spectra up to 1.0 GeV excitation energy. The solid lines correspond to the results of our model. The shaded regions, whose size stands for the experimental uncertainty, represent the experimental data. The dashed lines stand for experimental states whose mass is given but without indicating the error bars.

FIG. 3. $\Sigma^*(1/2^+)$ and $\Sigma(1/2^-)$ masses as a function of the cutoff masses of the one-pion and one-kaon exchanges, $\Lambda'_{\pi,K} = \Lambda_{\pi,K} + \Lambda_0$.

FIG. 4. $N(1/2^+)$, $\Xi(1/2^+)$, $\Delta(3/2^+)$ and $\Omega(3/2^+)$ ground state masses as a function of the regularization parameter \hat{r}_0 .

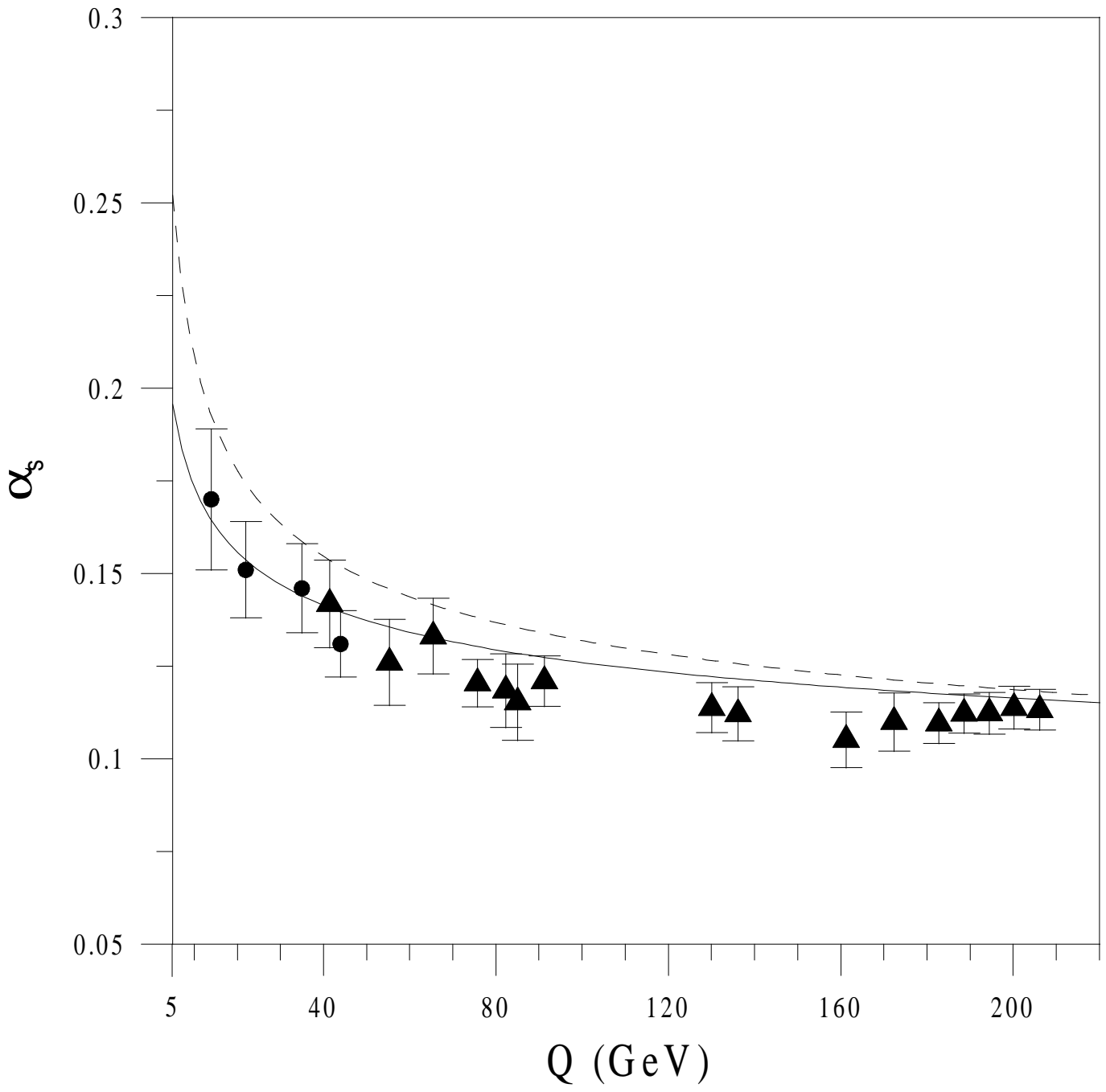


Figure 1

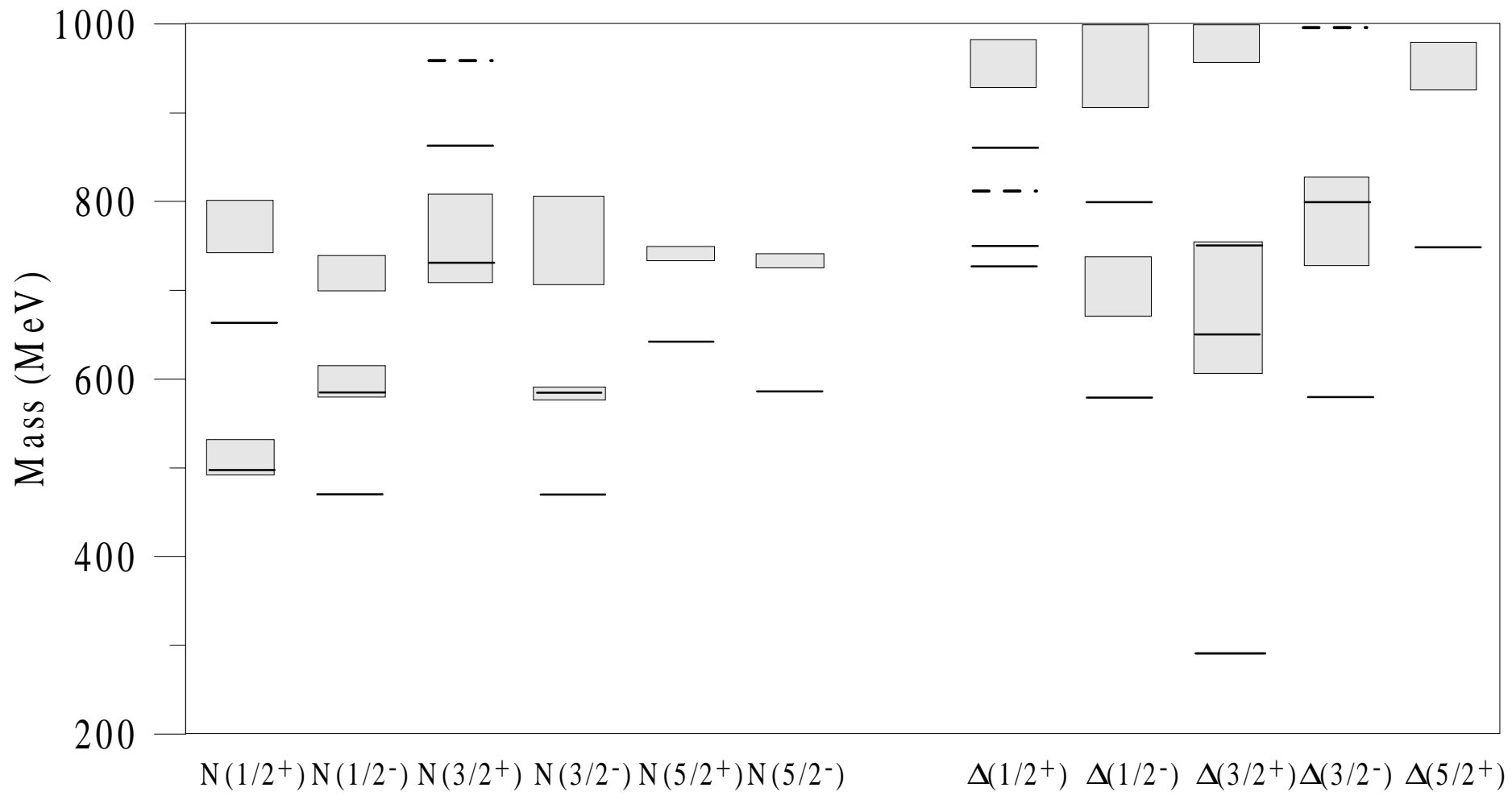


Figure 2 (a)

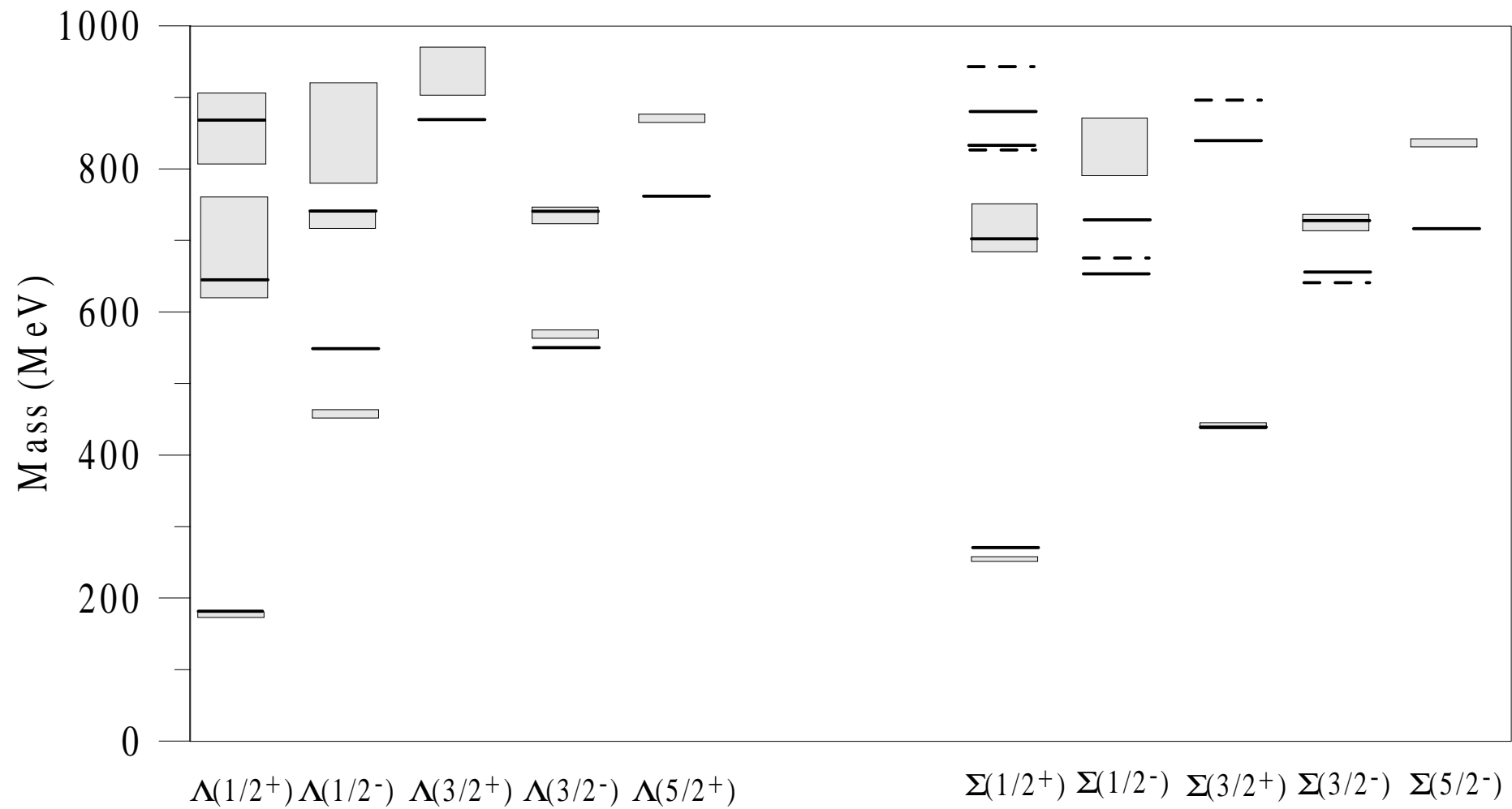


Figure 2 (b)

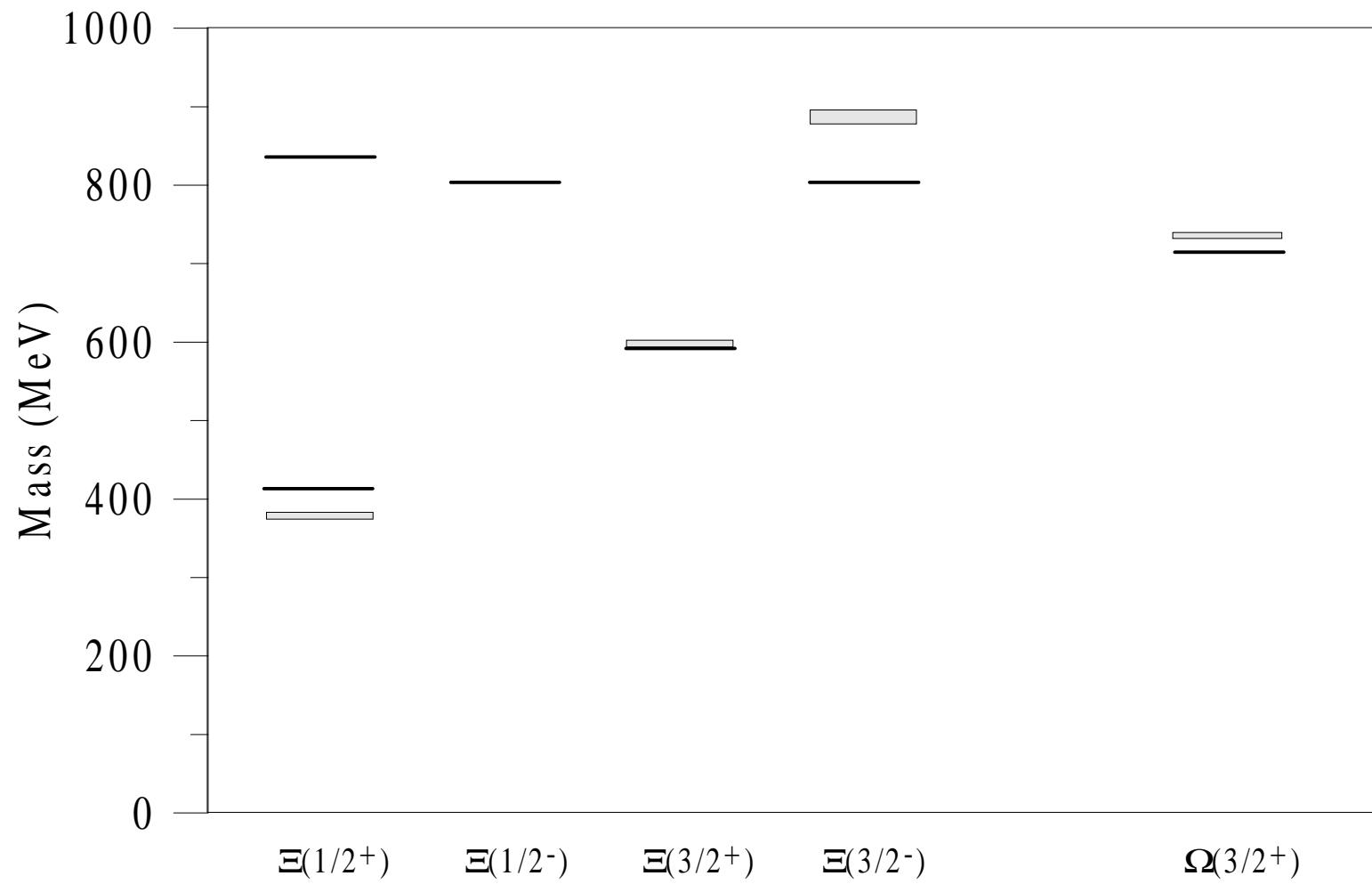


Figure 2 (c)

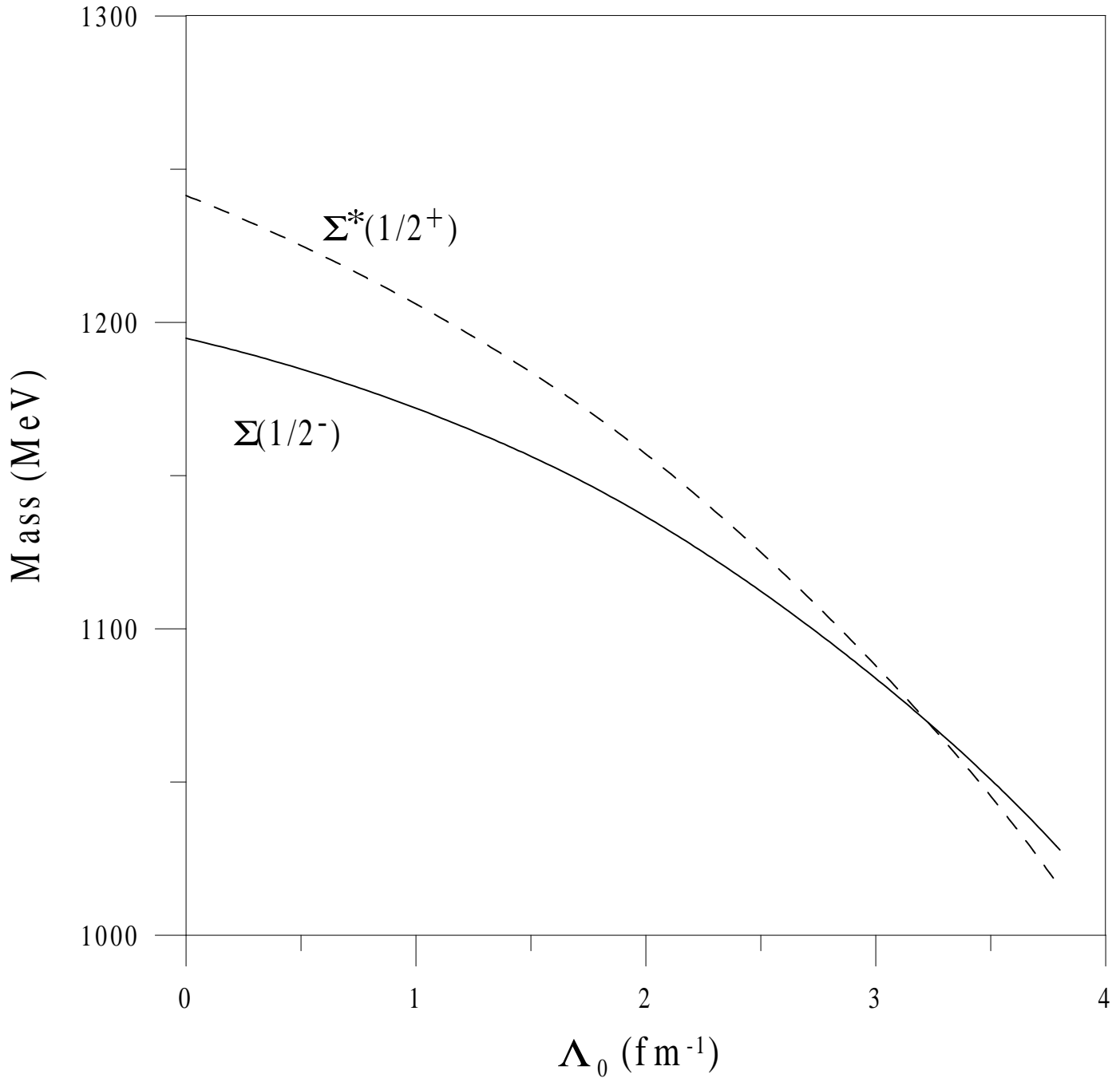


Figure 3

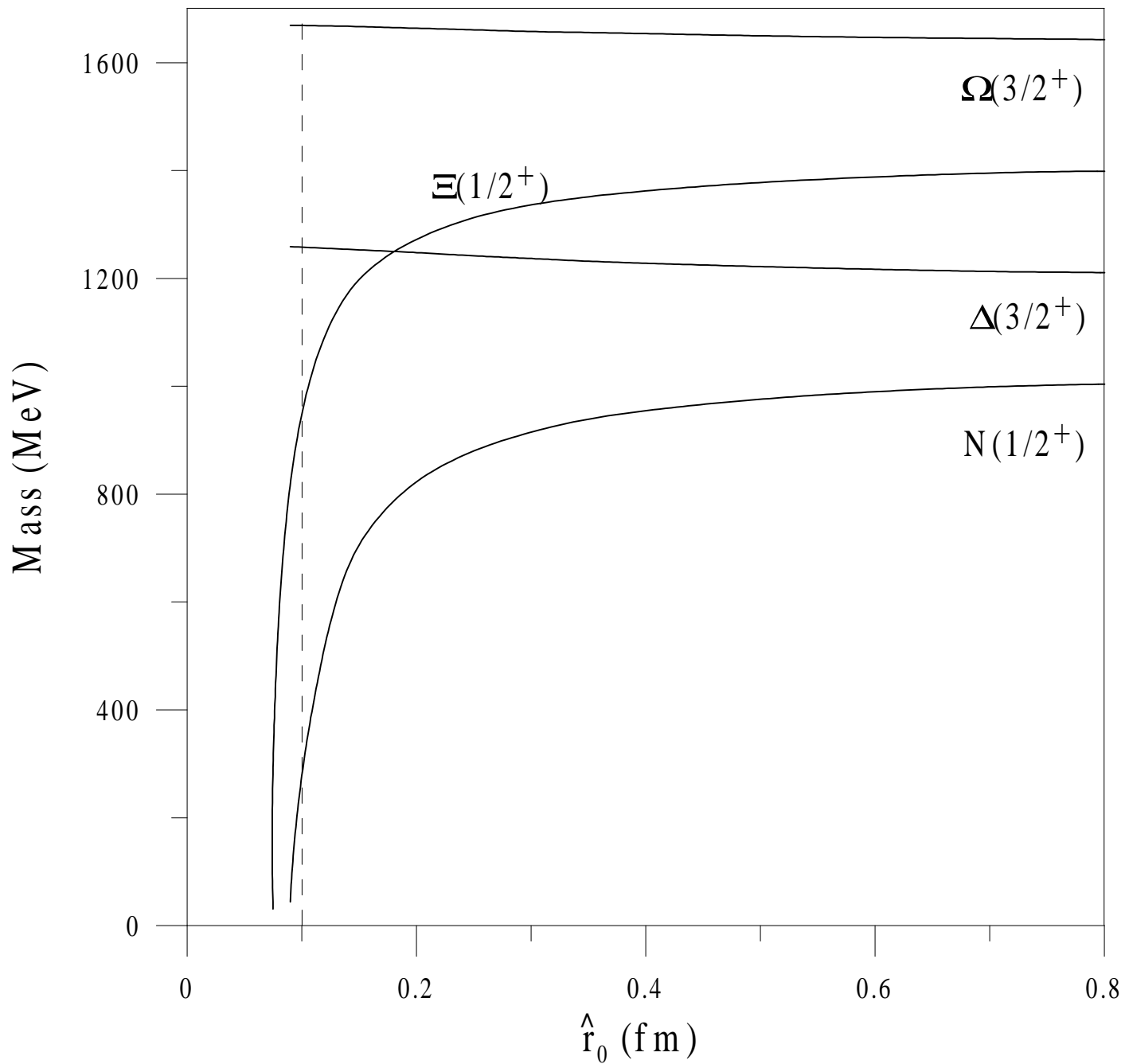


Figure 4